Pak. J. Bot., 57(6): 2033-2044, 2025. DOI: http://dx.doi.org/10.30848/PJB2025-6(42)

DIFFERENTIAL PHYSIOLOGICAL AND MOLECULAR RESPONSES OF FOUR TOBACCO GENOTYPES TO DROUGHT STRESS

LIYING YANG[1], GUOTAO JIA[2] AND ZHENG CHEN[1]*

[1]College of Tobacco Science, Henan Agricultural University, Zhengzhou 450002, China
[2]China Tobacco Henan Industry Co., Ltd. Zhengzhou, 450000, China
**Corresponding author's email: zhengchen@henau.edu.cn*

Abstract

Drought stress constitutes a critical environmental constraint limiting plant productivity worldwide. This study elucidates genotype-specific drought adaptation mechanisms in *Nicotiana tabacum* through integrated physiological, biochemical, and molecular analyses of four commercially significant cultivars (Y6, Y10, Y87, Hongda) exhibiting contrasting drought tolerance. PEG-induced water deficit significantly altered biomass partitioning, photosynthetic efficiency, redox homeostasis, and stress-responsive gene expression across various genotypes. Drought-tolerant cultivars Y6 and Y10 demonstrated superior resilience through: (1) improved water retention capacity and delayed leaf senescence, (2) preserved chloroplast ultrastructure, (3) maintained photosynthetic activity under stress, and (4) bolstered antioxidant defense systems. Additionally, molecular profiling revealed coordinated upregulation of ABA signaling (*NtNCED1*, *NtRD29A*), ROS scavenging (*NtSOD*, *NtCAT*), and osmoprotectant biosynthesis (*NtP5CS1*) genes in tolerant cultivars. This study introduces a mechanistic model that delineates multi-level adaptation strategies, where tolerant genotypes employ root architectural plasticity, non-stomatal photosynthetic maintenance, and antioxidant-genic synergy to mitigate dehydration damage. This systematic characterization of natural genetic variation provides actionable targets for the molecular breeding of drought-resistant tobacco cultivars.

Key words: Antioxidant defense; Drought; Gene expression; *Nicotiana tabacum*; Oxidative damage

Introduction

Global agricultural productivity faces escalating threats from environmental stressors, with drought emerging as a primary constraint due to its widespread occurrence and devastating impact on crop yields (Li *et al.*, 2021). Water deficit disrupts fundamental plant processes including growth regulation, photosynthetic efficiency, metabolic homeostasis, and transcriptional reprogramming (Alafari *et al.*, 2024). To mitigate these effects, plants deploy multifaceted adaptive strategies involving physiological adjustments, biochemical modifications, and molecular adaptations—a suite of responses that collectively determine drought tolerance (le Roux *et al.*, 2021; Meng *et al.*, 2022; dos Santos *et al.*, 2023). Understanding these mechanisms is crucial for maintaining food security amid climate change.

Nicotiana tabacum serves as both a model organism and a high-value leaf-harvested commercial crop globally (Chen *et al.*, 2021; Xu *et al.*, 2022). While substantial research has focused on enhancing disease resistance, abiotic stress tolerance, and secondary metabolite profiles in transgenic lines (Bao *et al.*, 2017; Ma *et al.*, 2017), critical knowledge gaps persist regarding natural genetic variation in drought response mechanisms, particularly those governing tobacco-specific adaptations. This oversight is concerning given tobacco's sensitivity to water deficits during its vegetative growth phase—stress events that impair biomass accumulation and trigger commercially critical shifts in carbon-nitrogen partitioning (e.g., sugar/nicotine balance) that compromise leaf quality (Su *et al.*, 2017).

Developing drought-resilient cultivars requires systematic evaluation of genotype-specific adaptation strategies—a challenge compounded by the polygenic nature of drought tolerance (Hezema *et al.*, 2021; Melandri *et al.*, 2021). Despite tobacco's agronomic importance and genomic resources, comparative analyses of natural genetic variation across the physiological-to-molecular continuum remain relatively scarce. Investigating the desiccation-tolerance mechanisms in tobacco plants could facilitate a better understanding of the genetic basis of drought tolerance, thus enabling the effective use of drought-resistant materials approach to enhance their drought tolerance.

This study utilizes a multi-level comparative approach to dissect drought adaptation strategies in four commercially significant tobacco cultivars (Y6, Y10, Y87, Hongda) with established differential drought tolerance (Y6/Y10: tolerant; Y87/Hongda: sensitive). Through integrated phenotypic, physiological, ultrastructural, and molecular analyses, we: (1) characterize genotype-specific responses to PEG-induced osmotic stress, (2) identify key markers of drought resilience, and (3) elucidate transcriptional regulation underlying stress adaptation. The findings provide a mechanistic framework for selecting drought-tolerant genotypes and inform strategies for improving water-use efficiency in tobacco cultivation systems.

Materials and Methods

Plant materials and stress treatments: Four commercially significant flue-cured tobacco (*Nicotiana tabacum* L.) cultivars, Yuyan6 (Y6), Yuyan10 (Y10), Yunyan87 (Y87), and Honghuadajinyuan (Hongda), were utilized in this study. Seeds were surface-sterilized with 30% (v/v) H_2O_2 for 10 min, rinsed thrice (1 min each) with sterile distilled water, and imbibed overnight. Germination proceeded on moist filter paper in darkness at 25°C for 6 days. Uniform seedlings were transplanted into 85 × 100 × 95 mm pots containing nutrient soil:vermiculite (1:1, v/v) under controlled conditions (16/8 h photoperiod, 25°C/18°C day/night, 200 $\mu mol \cdot m^{-2} \cdot s^{-1}$ PAR, 60% RH). At the three-leaf stage, plants were transferred to hydroponic systems containing ½-strength Hoagland solution (Fig. 1).

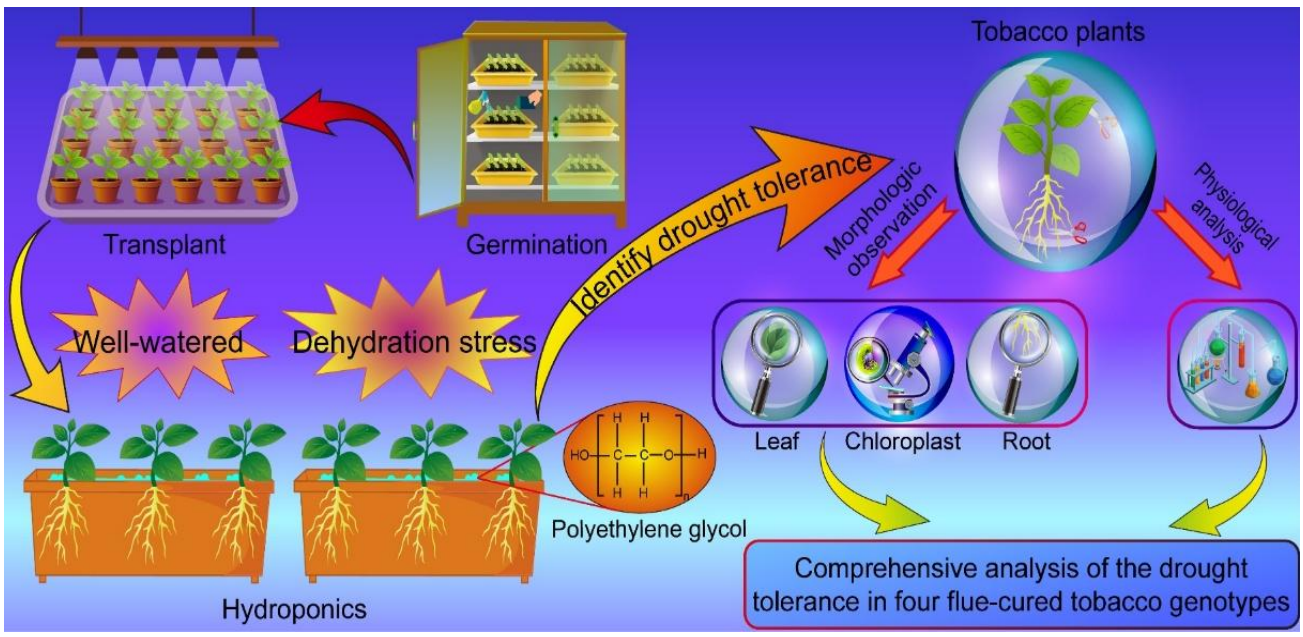

Fig 1. A schematic diagram of the experimental design and treatments.

Drought stress was imposed at the five-leaf stage by supplementing nutrient solution with 15% (w/v) polyethylene glycol (PEG, Ψ = -0.8 MPa), while controls received PEG-free solution. The experiment followed a randomized complete block design with three biological replicates (n = 3 plants per treatment). After 48 h stress exposure, the youngest fully expanded leaves were flash-frozen in liquid N_2 and stored at -80°C for downstream analyses.

Biomass and hydration status analysis: Plant biomass was measured following Qin *et al*., (2025). The leaf water potential (LWP) was verified concerning Hamzelou *et al*., (2020). The leaf relative water content (RWC) was estimated according to the method of Wang et al (2022). The rate of water loss from excised leaf was calculated as described by Dong *et al*., (2008). Ion leakage was measured using the method described by Gong *et al*., (2020). Chlorophyll content was determined as reported by Li *et al*., (2022).

Leaf ultrastructural analysis: For stomatal characterization, leaf abaxial surfaces were gold-sputtered (EM ACE600, Leica) and imaged using SU8010 SEM (Hitachi, Japan). Stomatal density and aperture were quantified from ≥10 fields per sample using ImageJ. Chloroplast ultrastructure was examined by H-7650 TEM (Hitachi, Japan) following glutaraldehyde-osmium fixation and uranyl acetate staining.

Photosynthetic parameter quantification: The net photosynthetic rate (Pn), transpiration rate (Tr), stomata conductance (Gs), and intercellular CO_2 concentration (Ci) were measured between 09:00~11:00 AM using a LI-6400 portable photosynthetic analyzer (LI-COR, USA) under the conditions described by Zhu et al (2022). Five measurements per plant were recorded on the second fully expanded leaf.

Biochemical determination and histochemical staining: Malondialdehyde (MDA) was quantified via thiobarbituric acid reaction. Superoxide radical ($O_2^{\bullet-}$) production rate was determined using hydroxylamine oxidation, while H_2O_2 content was measured via titanium sulfate method. The activities of antioxidant enzymes (SOD, POD, CAT, and APX) were measured according to the method determined using the appropriate detection kits (Jiancheng Bioengineering Institute, Nanjing, China) following the manufacturer's instructions. Relative electrical conductivity (REC) was measured by the conductance method. The insitu accumulation of $O_2^{\bullet-}$ and H_2O_2 was detected by staining with nitroblue tetrazolium (NBT) and diaminobenzidine (DAB), respectively. Production of superoxide anions in tobacco leaves was detected by the fluorescent dihydroethidium (DHE) probe, and apoptosis was detected by the fluorescent dye DAPI (4',6-diamidino-2-phenylindole) and TUNEL (TdT-mediated dUTP nick end labeling). In these experiments, the collection of leaf samples at indicated time was performed as soon as possible, and each independent assay was repeated at least three times.

Gene expression profiling: Total RNA was extracted using RNAprep Pure Plant Kit (DP441, Tiangen). First-strand cDNA synthesis employed PrimeScript RT Master Mix (RR036A, Takara). Transcript levels of genes were determined by qPCR using a Bio-Rad CFX96TM Real-Time PCR Detection System (USA) with gene-specific primers (Supplementary Table S1). Relative expression was calculated by $2^{-\Delta\Delta CT}$ method using *NtActin* (GenBank: AB158612) for normalization (Arocho *et al*., 2006). Three technical replicates per biological sample (n = 3) were analyzed.

Statistical analysis

Data represent mean ± SD (n≥3). Between-group differences were assessed by Student's t-test using SPSS 23.0. Significance thresholds were set at $*P<0.05$ and $**P<0.01$. Figures were generated with GraphPad Prism 9.0.

Supplementary Table 1. Primer sequences used for RT-qPCR analysis in this study.

Gene	Forward sequences (5' to 3')	Reverse sequences (5' to 3')
NtActin	CTATTCTCCGCTTTGGACTTGGCA	ACCTGCTGGAAGGTGCTGAGGGAA
NtNCED1	AAGAATGGCTCCGCAAGTTA	GCCTAGCAATTCCAGAGTGG
NtRD29A	TCGGTGTACCAACAGGCATA	CCCTTGCTTTGGTGTTGTTT
NtDREB	GCCGGAATACACAGGAGAAG	CCAATTTGGGAACACTGAGG
NtLTP1	GCAGAAGCCATAACCTGTGG	CAGTGGAAGGGCTGATCTTG
NtSPSA	GAATTCAGGCGCTTCGTTGTCA	ACCCCTAGTTTCTCCAGTGA
NtP5CS1	ATCTTCTAGTTCTGTTGA	CTCTCCTTAATGTATGTG
NtADC1	CTTGCTGATTACCGCAATTTATC	TAGGATCAGCAGCCCCCATAGCC
NtSAMDC	CATTCACATTACCCCGGAAG	AGCAACATCAGCATGCAAAG
NtLEA5	TTGAATCTGGGGTTTTGGTT	GGAAGCATTGACGAGCTAGG
NtERD10C	AACGTGGAGGCTACAGATCG	GTTCCTCTTGGGCATGAGTT
NtERD10D	GAGGACACGGCTGTACCAGT	GCGCCACTTCCTCTGTCTT
NtSOD	CTCCTACCGTCGCCAAAT	GCCCAACCAAGAGAACCC
NtPOD	CTCCATTTCCATGACTGCTTTG	GTTGGGTGGTGAGGTCTTT
NtCAT	AGGTACCGCTCATTCACACC	AAGCAAGCTTTTGACCCAGA
NtAPX	GCTGGAGTTGTTGCTGTTGA	TGGTCAGAACCCTTGGTAGC
NtGST	CCCCTAGTTTGCTCCCTTCT	TTCTTAGCTGCCTCCTGCTC

Results

Dehydration effect on plant growth and water status in four cultivars: Systematic analysis of PEG-induced drought responses across four tobacco cultivars (Y6, Y10, Y87, and Hongda) revealed pronounced genotypic divergence. Distinct phenotypic divergences were observed within 48 h of stress imposition, Y87 and Hongda exhibited severe leaf wilting, while Y6 and Y10 maintained turgor (Fig. 2A-B). Dynamic leaf LWP, water loss rate, and relative water content results revealed better water status in Y6 and Y10 than in Y87 and Hongda under drought (Fig. 2C-E). Particularly, oxidative damage, indicated by electrolyte leakage under drought conditions, was higher in Y87 and Hongda than in Y6 and Y10 (Fig. 2G). PEG-induced stress reduced fresh weight and shoot dry weight, with Y87 and Hongda experiencing significant drops compared to Y6 and Y10, while Y6 showed no significant difference from the control after 2 days (Fig. 2F, H). In contrast, root dry weight did not decrease in any cultivar (Fig. 2K), and the root-shoot ratio increased in all plants after dehydration (Fig. 2L). Root morphology analysis under both well-watered and dry conditions showed Y6 and Y10 had significantly increased total root length, surface area, and volume, but reduced average root diameter. However, Y10 and Hongda exhibited poor root tolerance, demonstrating minimal or no increase in root morphology indices when subjected to drought (Fig. 2I, J, M, N).

Dehydration effect on ultrastructure in four cultivars: Stomatal dynamics analysis via SEM revealed genotype-specific responses. The result indicated that the average stoma opening width of Y6 and Y10 decreased faster than that of Y87 and Hongda (Fig. 3A, C). Additionally, Hongda exhibited significantly higher stomatal density under water stress compared to well-watered conditions (Fig. 3D), suggesting a greater susceptibility to dehydration. To further examine the effect of water stress on cellular ultrastructure, we monitored the ultrastructural alterations in chloroplasts. Under normal conditions, chloroplast shapes were similar among the four seedlings. After stress, Y87 and Hongda showed altered chloroplast shapes with a decrease in both the size and number of starch granules (Fig. 3B). Chloroplast length and width analysis confirmed more significant morphological changes in Y87 and Hongda (Fig. 3E, F). Chlorophyll content and chloroplast cell area occupancy results also indicated Y87 and Hongda's chloroplasts were more susceptible to dehydration stress, whereas Y6 and Y10's were less affected (Fig. 3G, H).

Dehydration effect on photosynthetic parameters in four cultivars: Photosynthetic performance under drought revealed striking cultivar differences (Fig. 4). No significant differences were found among the four plants under normal conditions. After 2 days of drought, Y87 and Hongda exhibited more substantial reductions in Pn (53% and 62%, respectively) than Y6 and Y10 (28% and 41%, respectively) (Fig. 4A).Tr in stressed seedlings decreased markedly on 48 h, yet Y6 and Y10 retained relatively higher values than Y87 and Hongda (Fig. 4B). Gs changes paralleled Pn and Tr trends but were less pronounced but in a smaller range (Fig. 4C). However, Ci increases in Y87 and Hongda after 2 days of dehydration were higher than in Y6 and Y10, inversely correlating with Pn, Tr, and Gs (Fig. 4D).

Dehydration effect on physiological traits in four cultivars: Physiological profiling revealed the unique oxidative management strategies. Compared to controls, PEG-treated Y87 and Hongda had higher increases in MDA, REC, $O_2^{\bullet-}$, and H_2O_2 levels than Y6 and Y10 (Fig. 5A, B, D, E), indicating more severe membrane damage upon dehydration. The DAB, NBT, and DHE staining revealed higher ROS accumulation in Y87 and Hongda than in Y6 and Y10 (Fig. 5C, F). The DAPI and TUNEI fluorescence staining revealed more severe cell damage in Y87 and Hongda under drought stress than in Y6 and Y10, with merged results linking damage closely to ROS production (Fig. 5F, G). Meanwhile, SOD, POD, CAT, and APX enzyme levels were significantly higher in Y6 and Y10 than in Y87 and Hongda during water stress (Fig. 5H-K), suggesting high antioxidant enzyme activity is beneficial for maintaining oxidative stability.

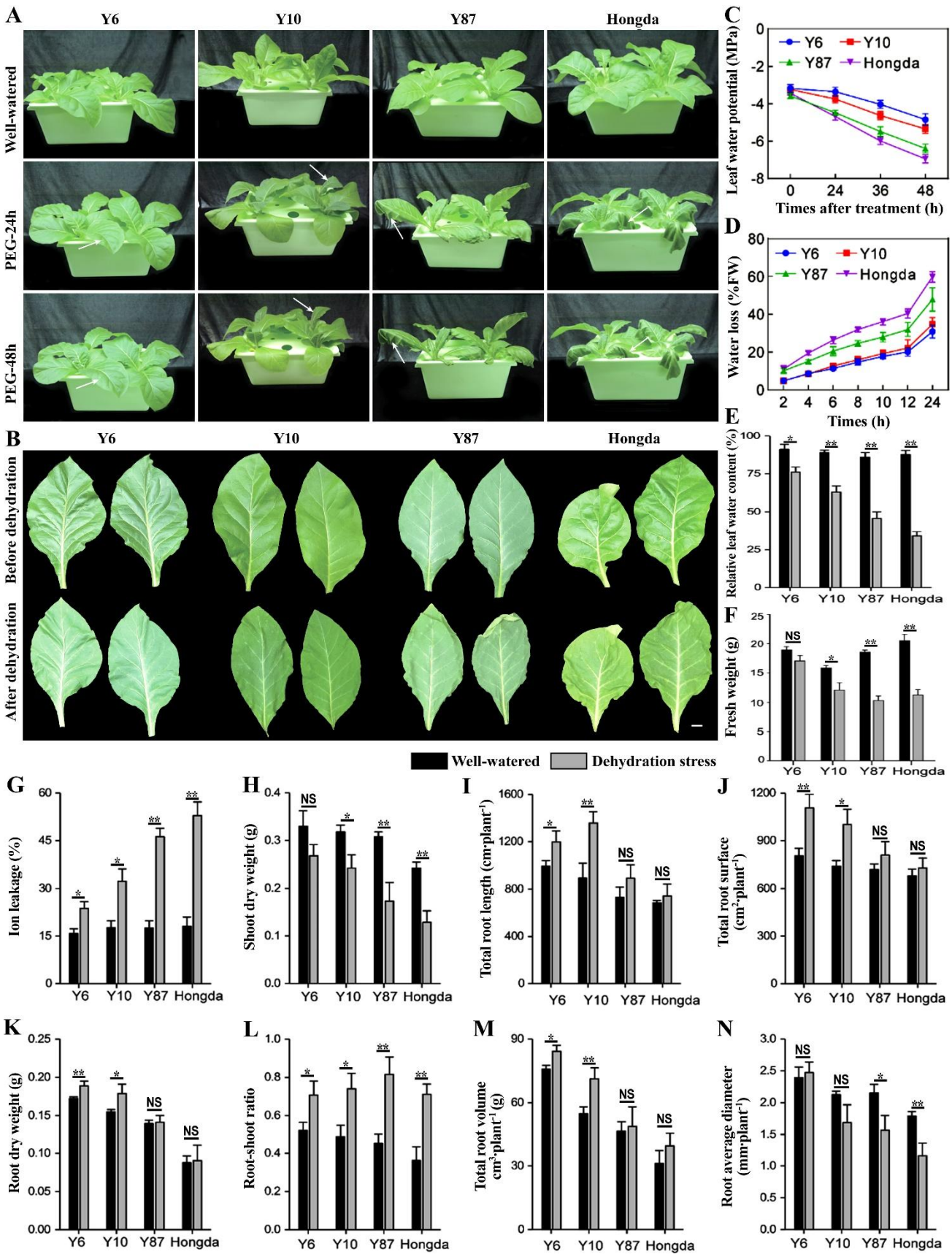

Fig. 2. Effects of dehydration stress on plant growth and water status in four tobacco cultivars. (**A**) The phenotypic change of four plants under normal conditions and drought stress; (**B**) Water loss phenotype in isolated leaves; (**C**) Leaf water potential; (**D**) Leaf water loss rate; I Relative leaf water content; (**F**) Fresh weight; (**G**) Ion leakage ratio; (**H**) Shoot dry weight; (**I**) Total root length; (**J**) Total root surface area; (**K**) Root dry weight; (**L**) Root-shoot ratio; (**M**) Total root volume; (**N**) Root average diameter. Values are expressed as means ± SE calculated from at least three independent experiments. Asterisks denote significant differences between the well-watered and dehydration stress conditions determined by Student's t-tests (**P*<0.05; ***P*<0.01). The same is below.

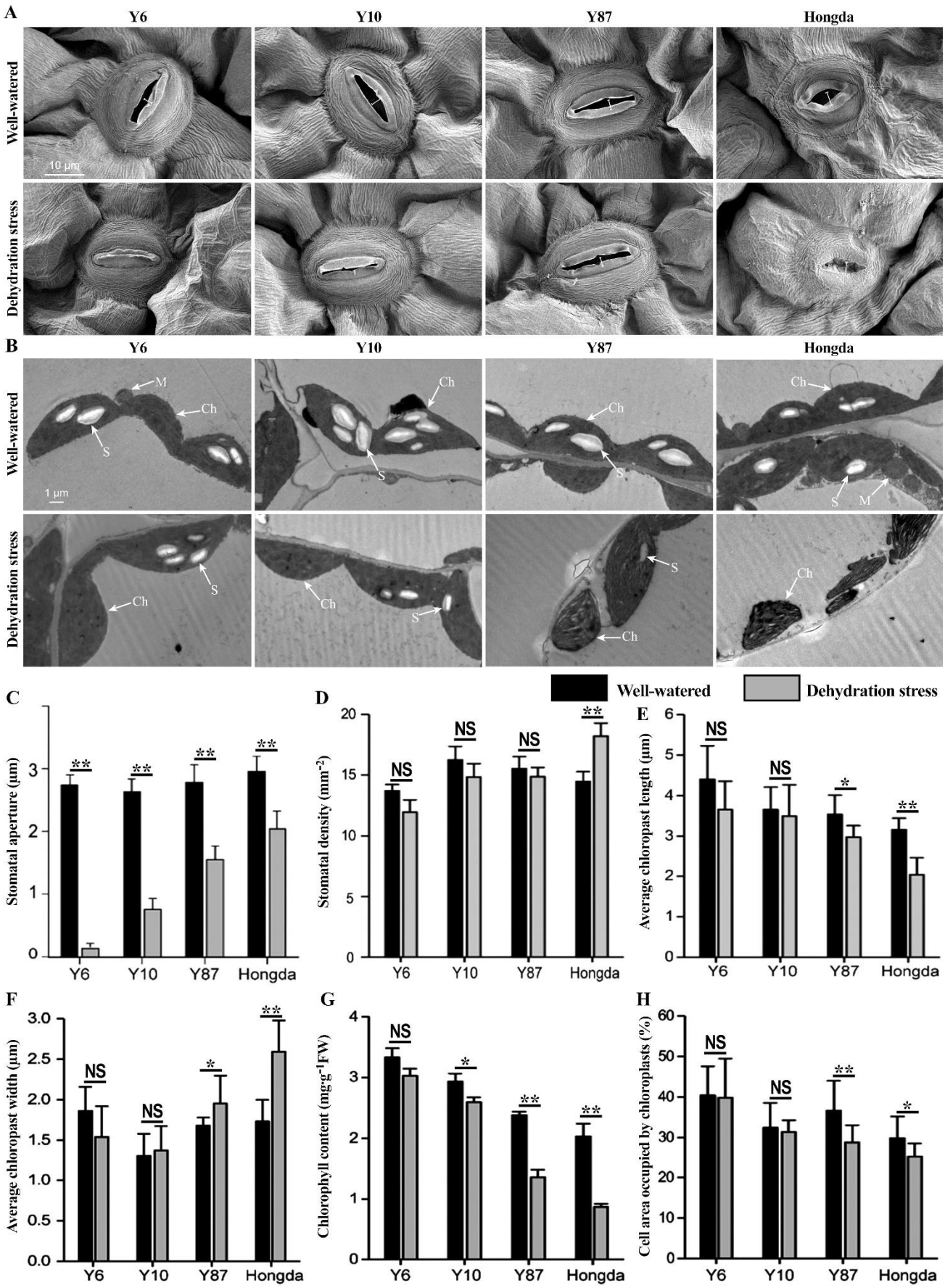

Fig 3. Changes in stomatal state and chloroplast ultrastructure after dehydration stress. (**A**) Scanning electron micrographs of stomata. (**B**) Scanning electron micrographs of chloroplast. Ch chloroplast; M mitochondria; S starch grain. (**C**) Analyses of stomata aperture. (**D**) Analyses of stomatal density. (**E**) Average length of chloroplast. (**F**) Average width of chloroplast. (**G**) Chlorophyll content. (**H**) Cell area occupied by chloroplasts. Bars represent mean ± SE calculated from at least fifteen replicates.

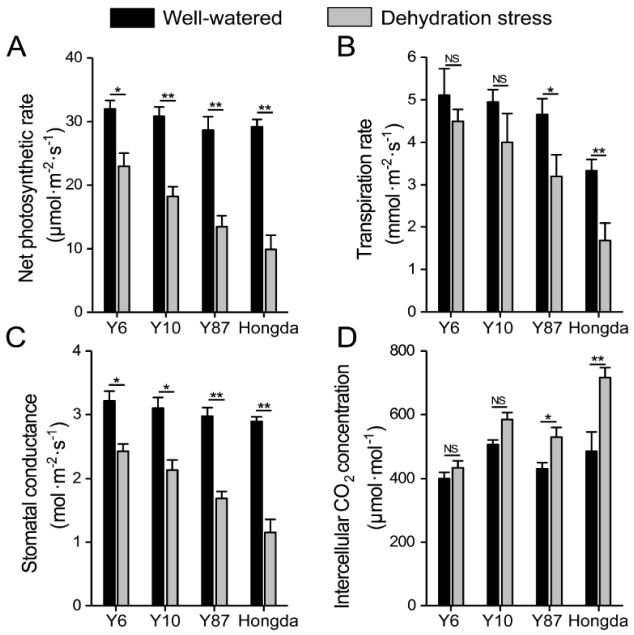

Fig 4. Changes of photosynthetic parameters in four types of tobacco plants under drought. (**A**) Net photosynthetic rate; (**B**) Transpiration rate; (**C**) Stomatal conductance; (**D**) Intercellular CO_2 concentration.

Dehydration effect on expression of stress-related genes in four cultivars: qPCR analysis of 16 stress-responsive genes revealed coordinated transcriptional enhancement in tolerant cultivars (Fig. 6). These genes include ABA-related (*NtNCED1* and *NtRD29A*), transcription factor (*NtDREB*), lipid-transfer protein (*NtLTP1*), sucrose-phosphate synthase (*NtSPSA*), LEA protein family (*NtERD10C*, *NtERD10D*, and *NtLEA5*), proline and polyamine biosynthesis (*NtP5CS1*, *NtADC1*, and *NtSAMDC*), and ROS-scavenging enzyme genes (*NtSOD*, *NtPOD*, *NtCAT*, *NtAPX*, and *NtGST*). This study observed these genes were significantly upregulated in the four cultivars when exposed to PEG-induced dehydration stress. Most notably, these stress-responsive genes showed higher expression in Y6 and Y10 compared to those in Y87 and Hongda (Fig. 6), which explains the stress defense systems activated by water stress in the four cultivars.

Discussion

Genotype-specific water management strategies: Drought-resilient plants optimize tissue hydration through coordinated water retention or tolerance to low tissue water potential (Thomas *et al.*, 2023). This study establishes that leaf water status parameters — quantified by LWP (Fig. 2C), water loss rate (Fig. 2D), and RWC (Fig. 2E)—serves as a robust phenotypic marker for drought tolerance screening. Notably, Y6 and Y10 maintained higher RWC than Y87 and Hongda under stress (Fig. 2E), which is consistent with their superior biomass retention (Fig. 2F, H, K) and root morphological plasticity (Fig. 2I, J, M, N). These observations corroborate reports linking osmotic acclimation to root-shoot ratio optimization (Banik *et al.*, 2016), as evidenced by increase in root-shoot ratio across all cultivars (Fig. 2L).

Stoma regulation strategies have important implications for preventing water loss from plants via transpiration, thereby enabling plants resilience to osmotic stress induced by drought (Tian *et al.*, 2022). SEM analysis revealed that the drought stress induced by PEG triggered stomatal closure as a critical water conservation strategy, with genotype-specific closure kinetics (Fig. 3A, C). Quantitatively, Y6 and Y10 exhibited more significant reductions in stomatal aperture width compared to Y87 and Hongda within 48 hours of stress exposure (Fig. 3C). This accelerated closure correlated strongly with their superior water retention capacity, as evidenced lower leaf water loss rates (Fig. 2D) and maintained leaf turgidity (Fig. 2A). Crucially, the preserved chloroplast ultrastructure in Y6 and Y10—characterized by intact thylakoid membranes (Fig. 3B) and <5% reduction in the chloroplast-occupied cell area (Fig. 3H)—contrasted sharply with the starch granule depletion and disrupted envelope membranes observed in Y87 and Hongda (Fig. 3B). These findings align with mechanistic studies that associated delayed stomatal closure with ROS-mediated chloroplast degradation (Anjum *et al.*, 2011; Yang *et al.*, 2022), as oxidative damage typically initiates in the chloroplasts due to their high metabolic activity and photosensitivity. The abnormal chloroplast morphology (e.g., swelling, stromal vacuolization) was directly correlated with 40–50% growth impairment under water deficit (Shao et al., 2016; AlNeyadi *et al.*, 2024). Our data confirm that chloroplast integrity serves as a key indicator of drought tolerance, which reflects the ability of a genotype to coordinate water conservation with photosynthetic functionality.

Photosynthetic regulation under dehydration: The higher tolerance of plants to water stress may be related to the control of gas exchange by their stomata, and the effect of dehydration on photosynthetic performance can help to evaluate the drought resistance of plants (Novick *et al.*, 2016, Liu *et al.*, 2021). Generally, drought-induced photosynthetic inhibition arises from both stomatal and non-stomatal limitations, with genotypic divergence in their predominance (Rangani *et al.*, 2016). The stomatal factor refers to the reduced diffusion of CO_2 through the stomata to the mesophyll and the non-stomatal factor refers to the metabolic capacity for CO_2 fixation. The differential photosynthetic resilience observed between genotypes (Fig. 4A-D) reflects distinct stomatal versus metabolic limitations. The increased Ci in susceptible genotypes (Fig. 4D) indicates non-stomatal photosynthetic inhibition, possibly due to damage to the chloroplasts (Fig. 3B, G) and accumulation of ROS (Fig. 5A-G). This aligns with the 53~62% Pn reduction in Y87 and Hongda versus 18~28% in tolerant genotypes (Fig. 4A), consistent with their contrasting chlorophyll retention (Fig. 3G) and biomass outcomes (Fig. 2F, K H). Sekmen *et al*., (2012) reported that a decrease in consequent Gs and Tr are regulatory strategies in plants exposed to oxidative stress. The water starvation-induced reduction in Gs can be attributed to stomatal closure, subsequently reducing water loss through transpiration in tobacco plants. Our data clearly indicate that the reduction in gas exchange directly results from stoma closure in PEG-stressed seedlings, leading to a significant decrease in CO_2 assimilation and photosynthetic activity. Moreover, the alterations observed in Ci were inversely related to Pn, Tr, and

Gs following the drought. Compared to the normal state, Y87 and Hongda showed a significant increase in Ci during the stress state, but no significant increases were observed in Y6 and Y10 (Fig. 4D). This suggests that the reduction in photosynthesis in Y87 and Hongda was mainly due to non-stomatal factors. Similar studies were also reported by Su *et al*., (2017), photosynthetic performance, decreased significantly in drought-sensitive cultivars compared to drought-tolerant cultivars. These genotype-specific gas exchange patterns (Fig. 4A-D) offer valuable actionable criteria for drought-tolerant cultivar selection.

Antioxidant defense mechanisms under dehydration: Water deficit stress can induce oxidative damage, represented as membrane lipid peroxidation, electrolyte leakage, and ROS overproduction (Mo *et al.*, 2016; Mubashir *et al.*, 2023). Membrane lipid peroxidation is an efficient indicator of free radical formation in plants exposed to drought (Lin *et al.*, 2024). The change in MDA content is typical of plants under drought stress, with these changes typically associated with an increase in membrane lipid peroxidation (Zandalinas *et al.*, 2017; Shreya *et al.*, 2022). ROS, such as $O_2^{\bullet-}$ and H_2O_2, are toxic molecules that can cause oxidative damage on critical biomolecules such as, DNA, proteins, and membrane lipids The dramatic increase in ROS accumulation, regarded as 'the oxidative burst', is fundamental in the plant's response to abiotic stress (Choudhury *et al.*, 2017, Ondrasek *et al.*, 2022). In our results, lipid peroxidation levels were dramatically increased in Y87 and Hongda than in Y6 and Y10, suggesting that Y6 and Y10 had had a higher capacity to maintain cell membrane integrity (Fig. 5A, B). Conversely, MDA and ROS accumulation in Y87 and Hongda increased substantially during drought stress (Fig. 5A, D, E), indicating that Y87 and Hongda have a lower capacity to adapt their metabolism to oxidative stress compared to Y6 and Y10. Previous studies have shown that high antioxidant enzyme activities contribute to osmotic tolerance by bolstering the cellular defense mechanisms against the detrimental effects of ROS (Xu *et al.*, 2021). To avoid excessive accumulation of ROS, SOD, which is recognized as the 'first line of defense' against superoxide free radicals generated under stress conditions, catalyzes the dismutation of $O_2^{\bullet-}$ into O_2 and H_2O_2, thereby reducing the titer of activated oxygen molecules within the cell (Bose *et al.*, 2014; Zhai *et al.*, 2020). Our findings indicated that Y6 and Y10 have more efficient defense systems than Y87 and Hongda during drought since the constitutive levels of protective enzymes (SOD, POD, CAT, and APX) in Y6 and Y10 were significantly higher than those assayed in Y87 and Hongda (Fig. 5H-K). The difference in antioxidant defenses among the four tobacco cultivars under stress further demonstrates that variations in cultivar can profoundly and significantly impact plant stress tolerance.

Transcriptional changes of stress-related genes under dehydration stress: In higher plants, drought stress has been documented to regulate the expression profiles of a series of ROS- and stress-related genes at the transcriptional level (Zhu, 2016). It is reported that *NCED* encodes the rate-limiting enzyme that participated in ABA biosynthesis and metabolism, which is significantly up-regulated in plants when subjected to various environmental stresses (Zhang *et al.*, 2009; Kumar *et al.*, 2022). The transgenic plants that overexpress the *NCED* gene exhibited an increased accumulation of ABA and antioxidant enzyme activities, thereby improving their resistance to drought stress. Besides *NCED*, *RD29A,* which is involved in the downstream response, plays a key role in the ABA signaling pathway and is also significantly up-regulated under drought stress. In this study, ABA-mediated stomatal closure in Y6/Y10 aligned with *NtNCED1* induction, while *NtRD29A* amplified stress-responsive transcription (Fig. 2, Fig. 6). The transcription factor known as *DREB*, which specifically binds to dehydration-responsive elements, plays an indispensable role in plant stress responses. It has been reported to improve tolerance to drought, salt, and frost stress by activating stress-inducible target genes expression and osmolyte accumulation in transgenic plants (Maruyama *et al.*, 2009, Kudo *et al.*, 2017). The lipid-transfer protein *LTP* could be dramatically induced by various abiotic stresses, which is considered necessary to protect cell membranes from oxidative damage caused by stress conditions (Hu *et al.*, 2013). It is reported that *LTP*-overexpressing transgenic lines significantly enhanced the resistance to both drought and salt stress by reducing the transpiration rate and increasing the ROS-scavenging enzyme expression levels (Xu *et al.*, 2018). The *SPSA* gene has a critical role in catalyzing the biosynthesis of sucrose, which could regulate the osmotic potential of cells, thus maintaining osmotic balance under stress conditions (Feng *et al.*, 2019). The osmolyte biosynthetic genes (*ADC1*, *SAMDC,* and *P5CS1*) play predominant roles in the biosynthesis and accumulation of polyamines and proline, which stabilize the membrane structure by acting as osmotic regulators under unfavorable conditions (Rajasheker *et al.*, 2019; Ghosh *et al.*, 2021). Other types of genes such as *LEA5*, *ERD10C*, and *ERD10D*, which are part of the *LEA* protein family; up-regulated expression of these genes could maintain the stability of cell membranes and biomacromolecules by through the production of additional chaperones or protective proteins (Amara *et al.*, 2012). ROS-related genes (*SOD*, *POD*, *CAT*, *APX*, and *GST*) encode the antioxidant enzymes involved in the detoxification of reactive oxygen species, which are important regulatory molecules protecting plants from damage caused by abiotic stress (Liu *et al.*, 2018). Antioxidant gene synergy was evident through co-expression of *NtSOD*, *NtCAT*, and *NtAPX*, which mirrored elevated enzyme activities and reduced oxidative damage in tolerant cultivars (Fig 5, Fig 6). Overall, our qPCR data analysis indicated that in the case of plant water loss, all of the above genes were differentially expressed among the four cultivars, but the expressions of these genes were induced in Y6 and Y10 at a higher level than in Y87 and Hongda (Fig. 6), proving that Y6 and Y10 have higher drought tolerance under drought conditions. These results are broadly consistent with previous studies, in which transgenic tobacco plants generally exhibited higher tolerance to drought stress by upregulating the expression of such stress-related genes under water deficit (Wei *et al.*, 2017; Wang *et al.*, 2019). Notably, we identified *NtRD29A*, *NtERD10D*, *NtLEA5*, and *NtPOX* as drought-responsive genes exhibiting exclusive upregulation in Y6 and Y10 under dehydration. These promising candidates warrant further investigation as priority molecular targets for breeding programs.

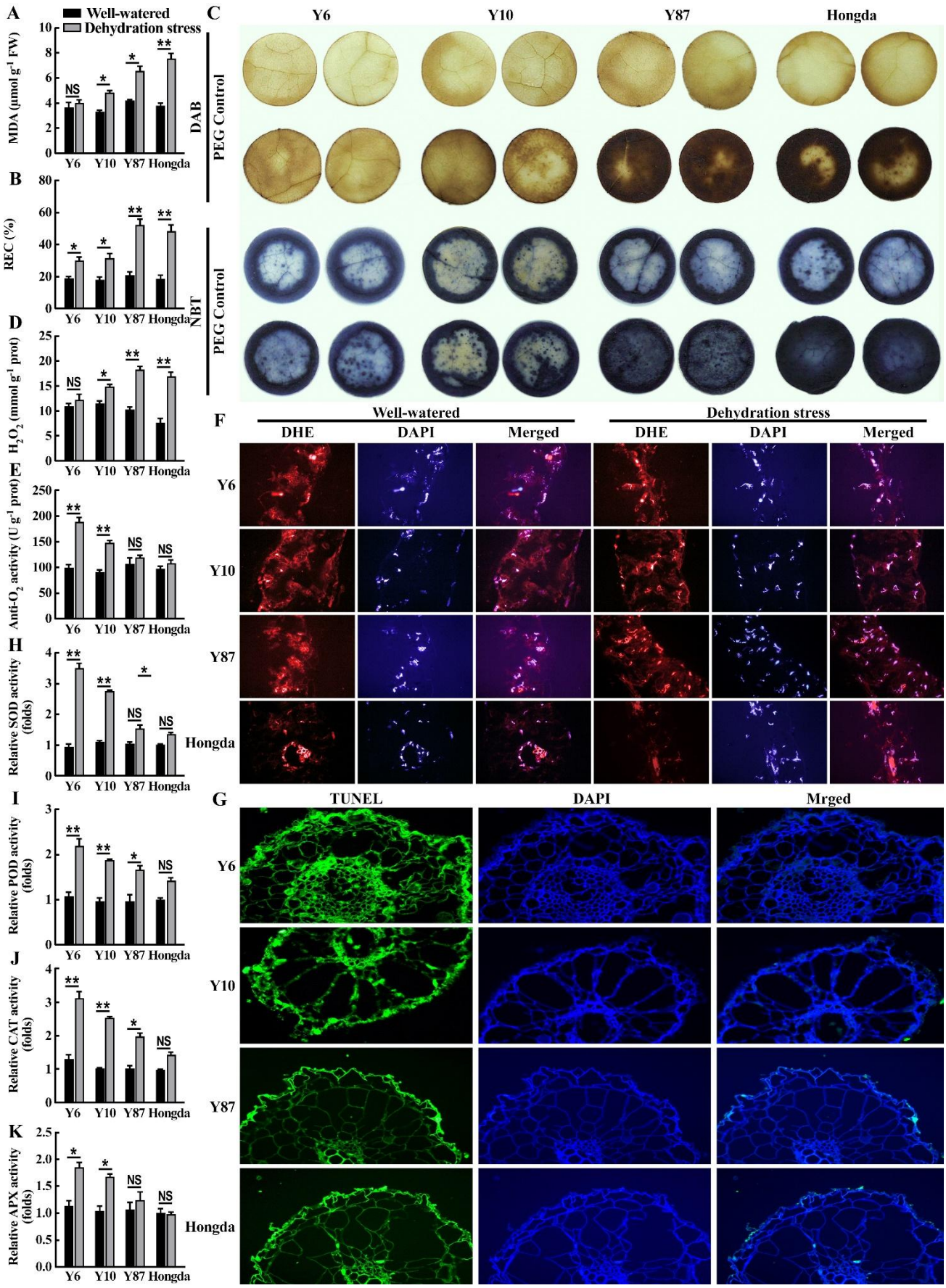

Fig 5. Biochemical changes in four types of tobacco plants under drought stress. (**A**, **B**, **D**, **E**) The indicators of oxidative damage (MDA, REC, H_2O_2, and $O_2^{\bullet-}$); (**C**) DAB and NBT leaf staining results; (**F**) DHE and DAPI treated tobacco leaves, and fluorescence photos were displayed in the merge mode; (**G**) TUNEL and DAPI treated tobacco root tips under PEG stress, and fluorescence images were displayed in the merge mode; (**H–K**) The activities of antioxidant enzymes (SOD, POD, CAT, and APX).

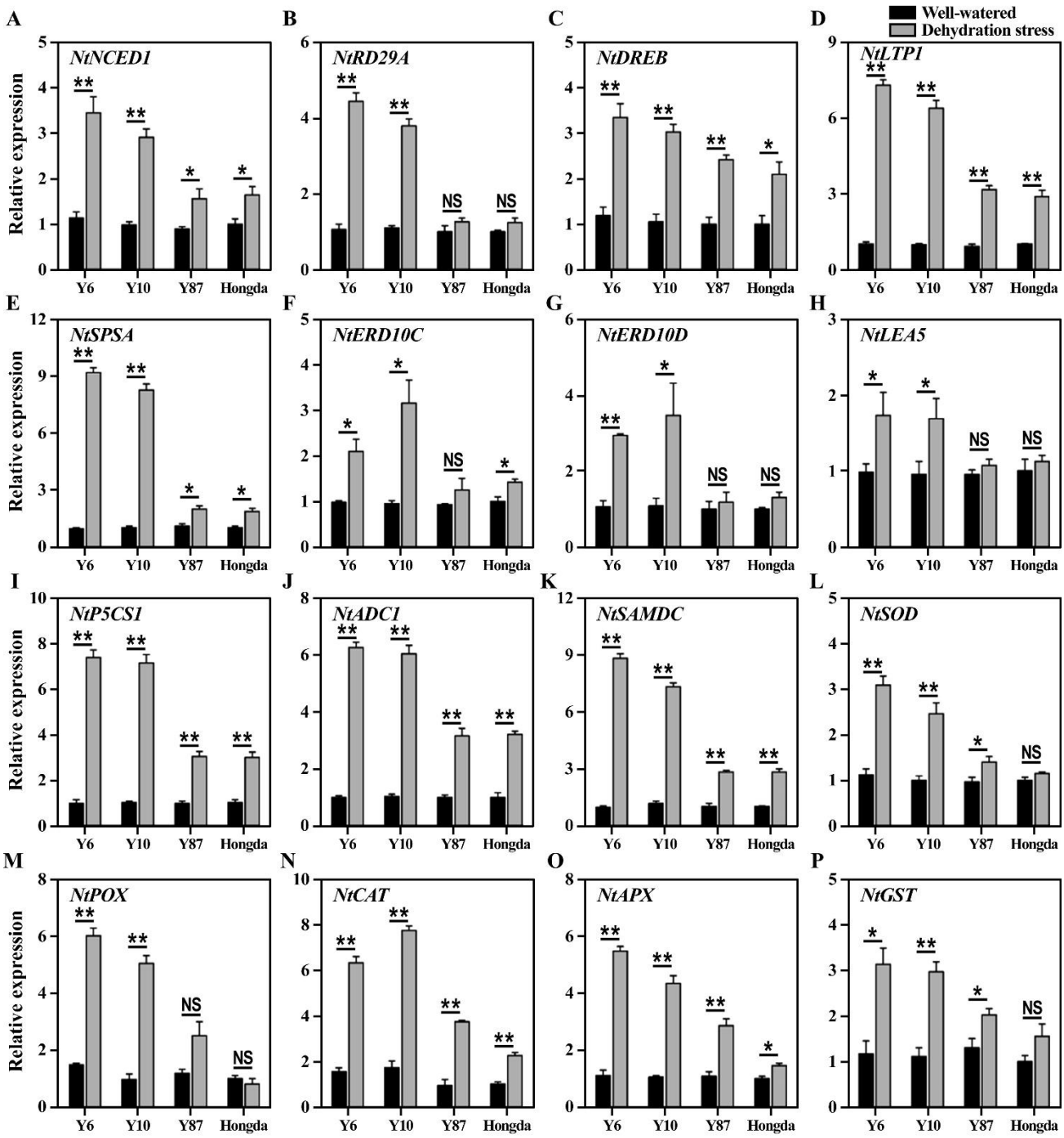

Fig 6. (**A–P**) qPCR analysis of stress-related genes in response to dehydration stress. For each assay, the expression level of Hongda under a well-watered condition was defined as 1.0.

Conclusions

This study comprehensively analyzed four tobacco cultivars' responses to drought stress, and proposed a model revealing the commonalities and differences of four tobacco cultivars in response to dehydration stress (Fig. 7). The proposed model illustrates that Y6 and Y10 had a better genetic basis against dehydration than Y87 and Hongda, as reflected in differences in physiological and molecular aspects. Compared to Y87 and Hongda, Y6 and Y10 had higher water retention capability, better photosynthetic performance, stronger antioxidant defenses, less oxidative damage, and higher expression of stress-related genes, resulting in better plant growth during drought. These traits associated with the increased expression of ABA signaling, ROS scavenging, and osmoprotectant biosynthesis genes. Notably, the balance between ROS production and antioxidant defense is vital for plant survival under drought conditions. The findings highlight the importance of root system adaptation, non-stomatal photosynthetic maintenance, and antioxidant synergies in drought resistance, providing a foundation for breeding drought-resistant tobacco varieties through targeted physiological and molecular traits. Future research should explore field conditions, hormonal interactions, and specific gene functions to deepen our understanding of drought tolerance mechanisms.

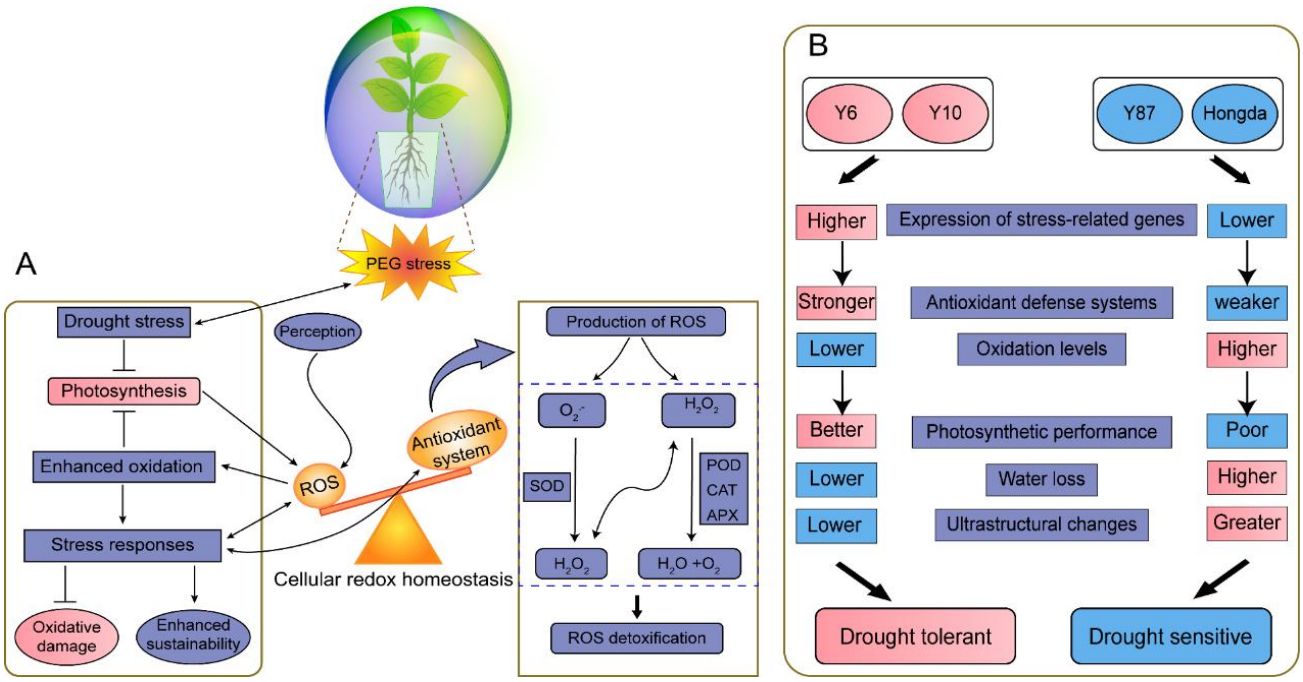

Fig 7. A model depicting (**A**) cellular redox state within the context of plants responding to PEG-induced dehydration stress and (**B**) drought tolerance of four tobacco cultivars under water deficit.

Funding

This project was financially supported by the Natural Science Foundation of Henan Province (No. 252300420183) and the Science & Technology Program of Henan Tobacco Industry (No. 2021410001300050).

References

Alafari, H.A., H. Freeg, M. Abdelrahman, K.A. Attia, A.S. Jalal, A. Ei-Banna, A. Aboshosha and S. Fiaz. 2024. Integrated analysis of yield response and early stage biochemical, molecular, and gene expression profiles of pre-breeding rice lines under water deficit stress. *Sci. Rep.*, 14(1): 17855.

AlNeyadi, S., S. Kappachery, T.A. Khan, S. Karumannil, M. AlHosani and M.A. Gururani. 2024. Ectopic expression of potato *ARP1* encoding auxin-repressed protein confers salinity stress tolerance in *Arabidopsis thaliana*. *Plos One*, 19(10): e0309452.

Amara, I., A. Odena, E. Oliveira, A. Moreno, K. Masmoudi, M. Pagès and A. Goday. 2012. Insights into maize LEA proteins: from proteomics to functional approaches. *Plant Cell Physiol.*, 53(2): 312-329.

Anjum, S.A., L.C. Wang, M. Farooq, M. Hussain, L.L. Xue and C.M. Zou. 2011. Brassinolide application improves the drought tolerance in maize through modulation of enzymatic antioxidants and leaf gas exchange. *J. Agron. Crop Sci.*, 197(3): 177-185.

Arocho, A., B. Chen, M. Ladanyi and Q. Pan. 2006. Validation of the 2-DeltaDeltaCt calculation as an alternate method of data analysis for quantitative PCR of BCR-ABL P210 transcripts. *Diagn. Mol. Pathol.*, 15(1): 56-61.

Banik, P., W. Zeng, H. Tai, B. Bizimungu and K. Tanino. 2016. Effects of drought acclimation on drought stress resistance in potato (*Solanum tuberosum* L.) genotypes. *Environ. Exp. Bot.*, 126: 76-89.

Bao, F., D. Du, Y. An, W. Yang, J. Wang, T. Cheng and Q. Zhang. 2017. Overexpression of *Prunus mume* dehydrin genes in tobacco enhances tolerance to cold and drought. *Front. Plant Sci.*, 8: 151.

Bose, J., A. Rodrigo-Moreno and S. Shabala. 2014. ROS homeostasis in halophytes in the context of salinity stress tolerance. *J. Exp. Bot.*, 65(5): 1241-1257.

Chen, Z., W. Jia, S. Li, J. Xu and Z. Xu. 2021. Enhancement of *Nicotiana tabacum* resistance against dehydration-induced leaf senescence via metabolite/phytohormone-gene regulatory networks modulated by melatonin. *Front. Plant Sci.*, 12: 686062.

Choudhury, F.K., R.M. Rivero, E. Blumwald and R. Mittler. 2017. Reactive oxygen species, abiotic stress and stress combination. *Plant J.*, 90(5): 856-867.

Dong, B., M. Liu, H. Shao, Q. Li, L. Shi, F. Du and Z. Zhang. 2008. Investigation on the relationship between leaf water use efficiency and physio-biochemical traits of winter wheat under rained condition. *Colloids Surf. B Biointer.*, 62(2): 280-287.

dos Santos, A.R., G.M.G. da Rocha, A.P. Machado, P.I. Fernandes-Junior, N.H.C. Arriel, T.M.S. Gondim and L.M. de Lima. 2023. Molecular and biochemical responses of sesame (*Sesamum indicum* L.) to rhizobacteria inoculation under water deficit. *Front. Plant Sci.*, 14: 1324643.

Feng, J., L. Wang, Y. Wu, Q. Luo, Y. Zhang, D. Qiu, J. Han, P. Su, Z. Xiong, J. Chang, G. Yang and G. He. 2019. *TaSnRK2.9*, a sucrose non-fermenting 1-related protein kinase gene, positively regulates plant response to drought and salt stress in transgenic tobacco. *Front. Plant Sci.*, 9: 2003.

Ghosh, U.K., M.N. Islam, M.N. Siddiqui and M.A.R. Khan. 2021. Understanding the roles of osmolytes for acclimatizing plants to changing environment: a review of potential mechanism. *Plant Signal. Behav.*, 16(8): 1913306.

Gong, W., B. Li, B. Zhang and W. Chen. 2020. ATG4 mediated Psm ES4326/*AvrRpt2*-induced autophagy dependent on salicylic acid in *Arabidopsis thaliana*. *Int. J. Mol. Sci.*, 21(14): 5147.

Hamzelou, S., K.S. Kamath, F. Masoomi-Aladizgeh, M.M. Johnsen, B.J. Atwell and P.A. Haynes. 2020. Wild and cultivated species of rice have distinctive proteomic responses to drought. *Int. J. Mol. Sci.*, 21(17): 5980.

Hezema, Y.S., M.R. Shukla, M.M. Ayyanath, S.M. Sherif and P.K. Saxena. 2021. Physiological and molecular responses of six apple rootstocks to osmotic stress. *Int. J. Mol. Sci.*, 22(15): 8263.

Hu, W., C. Huang, X. Deng, S. Zhou, L. Chen, Y. Li, C. Wang, Z. Ma, Q. Yuan, Y. Wang, R. Cai, X. Liang, G. Yang and G. He. 2013. TaASR1, a transcription factor gene in wheat, confers drought stress tolerance in transgenic tobacco. *Plant Cell Environ.*, 36(8): 1449-1464.

Kudo, M., S. Kidokoro, T. Yoshida, J. Mizoi, D. Todaka, A.R. Fernie, K. Shinozaki and K. Yamaguchi-Shinozaki. 2017. Double overexpression of DREB and PIF transcription factors improves drought stress tolerance and cell elongation in transgenic plants. *Plant Biotechnol. J.*, 15(4): 458-471.

Kumar, S., S.H. Shah, Y. Vimala, H.S. Jatav, P. Ahmad, Y. Chen and K.H.M. Siddique. 2022. Abscisic acid: Metabolism, transport, crosstalk with other plant growth regulators, and its role in heavy metal stress mitigation. *Front. Plant Sci.*, 13: 972856.

le Roux, M.S.L., N.F.V. Burger, M. Vlok, K.J. Kunert, C.A. Cullis and A.M. Botha. 2021. EMS derived wheat mutant BIG8-1 (*Triticum aestivum* L.) - a new drought tolerant mutant wheat line. *Int. J. Mol. Sci.*, 22(10): 5314.

Li, C., Y. Tang, F. Gu, X. Wang, W. Yang, Y. Han and Y. Ruan. 2022. Phytochemical analysis reveals an antioxidant defense response in *Lonicera japonica* to cadmium-induced oxidative stress. *Sci. Rep.*, 12(1): 6840.

Li, Z., M. Tang, B. Cheng and L. Han. 2021. Transcriptional regulation and stress-defensive key genes induced by γ-aminobutyric acid in association with tolerance to water stress in creeping bentgrass. *Plant Signal. Behav.*, 16(3): 1858247.

Lin, S., W. Zhang, G. Wang, Y. Hu, X. Zhong and G. Tang. 2024. Physiological regulation of photosynthetic-related indices, antioxidant defense, and proline anabolism on drought tolerance of wild soybean (*Glycine soja* L.). *Plants*, 13(6): 880.

Liu, B., L. Kong, Y. Zhang and Y. Liao. 2021. Gene and metabolite integration analysis through transcriptome and metabolome brings new insight into heat stress tolerance in potato (*Solanum tuberosum* L.). *Plants*, 10(1): 103.

Liu, C., Y. Xu, Y. Feng, D. Long, B. Cao, Z. Xiang and A. Zhao. 2018. Ectopic expression of mulberry G-proteins alters drought and salt stress tolerance in tobacco. *Int. J. Mol. Sci.*, 20(1): 89.

Ma, X., G. Wang, W. Zhao, M. Yang, N. Ma, F. Kong, X. Dong and Q. Meng. 2017. SlCOR413IM1: A novel cold-regulation gene from tomato, enhances drought stress tolerance in tobacco. *J. Plant Physiol.*, 216: 88-99.

Maruyama, K., M. Takeda, S. Kidokoro, K. Yamada, Y. Sakuma, K. Urano, M. Fujita, K. Yoshiwara, S. Matsukura, Y. Morishita, R. Sasaki, H. Suzuki, K. Saito, D. Shibata, K. Shinozaki and K.Y. Shinozaki. 2009. Metabolic pathways involved in cold acclimation identified by integrated analysis of metabolites and transcripts regulated by DREB1A and DREB2A. *Plant Physiol.*, 150(4): 1972-1980.

Melandri, G., K.R. Thorp, C. Broeckling, A.L. Thompson, L. Hinze and D. Pauli. 2021. Assessing drought and heat stress-induced changes in the cotton leaf metabolome and their relationship with hyperspectral reflectance. *Front. Plant Sci.*, 12: 751868.

Meng, H.L., P.Y. Sun, J.R. Wang, X.Q. Sun, C.Z. Zheng, T. Fan, Q.F. Chen and H.Y. Li. 2022. Comparative physiological, transcriptomic, and WGCNA analyses reveal the key genes and regulatory pathways associated with drought tolerance in Tartary buckwheat. *Front. Plant Sci.*, 13: 985088.

Mo, Y., Y. Wang, R. Yang, J. Zheng, C. Liu, H. Li, J. Ma, Y. Zhang, C. Wei and X. Zhang. 2016. Regulation of plant growth, photosynthesis, antioxidation and osmosis by an arbuscular mycorrhizal fungus in watermelon seedlings under well-watered and drought conditions. *Front. Plant Sci.*, 7: 644.

Mubashir, A., Z.U. Nisa, A.A. Shah, M. Kiran, I. Hussain, N. Ali, L. Zhang, M.M.Y. Madnay, W.A. Alsiary, S.M. Korany, M. Ashraf, B.A. Al-Mur and H. AbdElgawad. 2023. Effect of foliar application of nano-nutrients solution on growth and biochemical attributes of tomato (*Solanum lycopersicum*) under drought stress. *Front. Plant Sci.*, 13: 1066790.

Novick, K.A., C.F. Miniat and J.M. Vose. 2016. Drought limitations to leaf-level gas exchange: Results from a model linking stomatal optimization and cohesion-tension theory. *Plant Cell Environ.*, 39(3): 583-596.

Ondrasek, G., S. Rathod, K.K. Manohara, C. Gireesh, M.S. Anantha, A.S. Sakhare, B. Parmar, B.K. Yadav, N. Bandumula, F. Raihan, A.Z. Chmielewska, C.M. Gergichevich, M.R. Díaz, A. Khan, O. Panfilova, A.S. Fuentealba, S.M. Romero, B. Nabil, C.C. Wan, J. Shepherd and J. Horvatinec. 2022. Salt stress in plants and mitigation approaches. *Plants*, 11(6): 717.

Qin, M., J. Yan, R. Li, T. Jia, X. Sun, Z. Liu, M.A. El-Sheikh, P. Ahmad and P. Liu. 2025. Integrated physiological, transcriptomic, and metabolomic investigation reveals that MgO NPs mediate the alleviation of cadmium stress in tobacco seedlings through ABA-regulated lignin synthesis. *J. Hazard. Mater.*, 483: 136693.

Rajasheker, G., G. Jawahar, N. Jalaja, S.A. Kumar, P.H. Kumari, D.L. Punita, A.R. Karumanchi, P.S. Reddy, P. Rathnagiri, N. Sreenivasulu and P.B.K. Kishor. 2019. Role and regulation of osmolytes and ABA interaction in salt and drought stress tolerance. *Plant Signal. Mol.*, 417-436.

Rangani, J., A.K. Parida, A. Panda and A. Kumari. 2016. Coordinated changes in antioxidative enzymes protect the photosynthetic machinery from salinity induced oxidative damage and confer salt tolerance in an extreme halophyte *Salvadora persica* L. *Front. Plant Sci.*, 7: 50.

Sekmen, A.H., I. Turkan, Z.O. Tanyolac, C. Ozfidan and A. Dinc. 2012. Different antioxidant defense responses to salt stress during germination and vegetative stages of endemic halophyte Gypsophila oblanceolata Bark. *Environ. Exp. Bot.*, 77: 63-76.

Shao, R.X., L.F. Xin, H.F. Zheng, L.L. Li, Y.R. Zhang, Z.M. Hu and J. Zhang. 2016. Changes in chloroplast ultrastructure in leaves of drought-stressed maize inbred lines. *Photosynthetica*, 54(1): 74-80.

Shreya, S., L. Supriya and G. Padmaja. 2022. Melatonin induces drought tolerance by modulating lipoxygenase expression, redox homeostasis and photosynthetic efficiency in *Arachis hypogaea* L. *Front. Plant Sci.*, 13: 1069143.

Su, X., F. Wei, Y. Huo and Z. Xia. 2017. Comparative physiological and molecular analyses of two contrasting flue-cured tobacco genotypes under progressive drought stress. *Front. Plant Sci.*, 8: 827.

Thomas, F.M., L. Schunck and A. Zisakos. 2023. Legacy effects in buds and leaves of European beech saplings (*Fagus sylvatica*) after severe drought. *Plants*, 12(3): 568.

Tian, D., Q. Xie, Z. Deng, J. Xue, W. Li, Z. Zhang, Y. Dai, B. Zheng, T. Lu, I. De Smet and Y. Guo. 2022. Small secreted peptides encoded on the wheat (*Triticum aestivum* L.) genome and their potential roles in stress responses. *Front. Plant Sci.*, 13: 1000297.

Wang, H., M. Wang and Z. Xia. 2019. Overexpression of a maize SUMO conjugating enzyme gene (*ZmSCE1e*) increases sumoylation levels and enhances salt and drought tolerance in transgenic tobacco. *Plant Sci.*, 281: 113-121.

Wang, Z., Y. Jia, J. Fu, Z. Qu, X. Wang, D. Zou, J. Wang, H. Liu, H. Zheng, J. Wang, L. Yang, H. Xu and H. Zhao. 2022. An analysis based on japonica rice root characteristics and crop growth under the interaction of irrigation and nitrogen methods. *Front. Plant Sci.*, 13: 890983.

Wei, Q., Q. Luo, R. Wang, F. Zhang, Y. He, Y. Zhang, D. Qiu, K. Li, J. Chang, G. Yang and G. He. 2017. A wheat R2R3-type MYB transcription factor TaODORANT1 positively regulates drought and salt stress responses in transgenic tobacco plants. *Front. Plant Sci.*, 8: 1374.

Xu, J., M. Cai, J. Li, B. Chen, Z. Chen, W. Jia and Z. Xu. 2022. Physiological, biochemical and metabolomic mechanisms of mitigation of drought stress-induced tobacco growth inhibition by spermidine. *Ind. Crop Prod.*, 181: 114844.

Xu, X., Y. Zhou, P. Mi, J. Chen, W. Yang, T. Ma, J. Li, J. Zhang, L. Xu, X. Zhang and F. Chen. 2021. Salt-tolerance screening in *Limonium sinuatum* varieties with different flower colors. *Sci. Rep.*, 11: 14562.

Xu, Y., X. Zheng, Y. Song, L. Zhu, Z. Yu, L. Li, M. Zhang and G. Liu. 2018. NtLTP4, a lipid transfer protein that enhances salt and drought stress tolerance in *Nicotiana tabacum*. *Sci. Rep.*, 8: 8873.

Yang, X., Y. Han, J. Hao, X. Qin, C. Liu and S. Fan. 2022. Exogenous spermidine enhances the photosynthesis and ultrastructure of lettuce seedlings under high-temperature stress. *Sci. Hort.*, 291: 110570.

Zandalinas, S.I., D. Balfagón, V. Arbona and A. Gómez-Cadenas. 2017. Modulation of antioxidant defense system is associated with combined drought and heat stress tolerance in citrus. *Front. Plant Sci.*, 8: 953.

Zhai, K., G. Zhao, H. Jiang, C. Sun and J. Ren. 2020. Overexpression of maize *ZmMYB59* gene plays a negative regulatory role in seed germination in *Nicotiana tabacum* and *Oryza sativa*. *Front. Plant Sci.*, 11: 564665.

Zhang, Y., J. Tan, Z. Guo, S. Lu, S. He, W. Shu and B. Zhou. 2009. Increased abscisic acid levels in transgenic tobacco over-expressing 9 cis-epoxycarotenoid dioxygenase influence H_2O_2 and NO production and antioxidant defences. *Plant Cell Environ.*, 32(5): 509-519.

Zhu, C., H. Luo, L. Luo, K. Wang, Y. Liao, S. Zhang, S. Huang, X. Guo and L. Zhang. 2022. Nitrogen and biochar addition affected plant traits and nitrous oxide emission from *Cinnamomum camphora*. *Front. Plant Sci.*, 13: 905537.

Zhu, J.K. 2016. Abiotic stress signaling and responses in plants. *Cell*, 167(2): 313-324.

(Received for publication 9 April 2025)